Applied Catalysis B: Environmental 115–116 (2012) 209–218

Contents lists available at SciVerse ScienceDirect

Applied Catalysis B: Environmental

journal homepage: www.elsevier.com/locate/apcatb

A parametric study of the UV-A photocatalytic oxidation of H_2S over TiO_2

Angela Alonso-Tellez[a], Didier Robert[a,b], Nicolas Keller[a], Valérie Keller[a,*]

[a] Laboratoire des Matériaux, Surfaces et Procédés pour la Catalyse (LMSPC), CNRS, University of Strasbourg, 25 rue Becquerel 67087, Strasbourg, France
[b] Saint-Avold Antenna, LMSPC, CNRS, University of Metz and University of Strasbourg, rue Victor Demange, 57500 Saint-Avold, France

ARTICLE INFO

Article history:
Received 25 August 2011
Received in revised form 4 December 2011
Accepted 9 December 2011
Available online 17 December 2011

Keywords:
TiO_2
Hydrogen sulfide
Photocatalysis
Sulfates
Parametric study
Regeneration
XPS surface analysis
Reaction mechanisms

ABSTRACT

A parametric study of the UV-A H_2S photocatalytic oxidation over TiO_2 P25 has investigated the influence of the TiO_2 coating surface density, the total flow rate, the relative humidity, the temperature and the irradiance as main reaction parameters on the H_2S conversion, the SO_2 selectivity (targeted as low as possible), the duration without any SO_2 release, and thus on the gas phase sulfur removal efficiency. The deepest non-illuminated internal TiO_2 layers – even not photocatalytically active – could play a role in adsorbing SO_2 and delaying its release into the gas phase, for explaining the behavior of high surface density TiO_2 coatings. The Ti^{4+} surface sites have been proposed to act as active sites for the H_2S photocatalytic oxidation, and general reaction pathways leading to the formation of SO_2 in the gas phase and to surface sulfates have been hypothesized, involving photogenerated holes, sulfhydryl radicals or hydroxyl radicals. The role of active sulfate radicals has been put forward for explaining the behavior turn with time on stream on sulfate-deactivated TiO_2, from a progressive deactivation into a complete H_2S conversion to SO_2. Finally, effective regeneration treatment with recovering of the initial activity could be performed by weakly basic washing.

1. Introduction

Hydrogen sulfide (H_2S) is a malodorous, toxic and corrosive compound, with a 0.0004 ppm low odor threshold and a characteristic rotten-egg smell [1,2], emitted from wastewater treatment or released as by-product of processes like petroleum refining, pulp and paper manufacturing, Treating H_2S-containing air is important for environmental reasons (acid rain precursor contributing to global warming) and maintenance problematic (corrosive attack on process equipment), as well as for public concern over human health and comfort (noxious and nasty odor) in the frame of the indoor air quality control.

Therefore, removing H_2S from air remains a relevant issue, the main actual processes being biofiltration, thermal incineration combined with catalytic processes and wet scrubbing. The works devoted to the photocatalysis degradation of H_2S remained scarce by contrast to those on the mineralization of hazardous organic molecules. However, photocatalysis was reported to be efficient for removing H_2S from air, with the formation of sulfates as ultimate reaction products accumulating at the catalyst surface. This causes an inherent primary problem and leads to *on-flow* deactivation [3–12]. The mechanism of the H_2S photocatalytic oxidation remains not fully understood. Reaction pathways involving SO_2 as oxidation intermediate [9–11] and/or the direct formation of sulfates from H_2S through an eight-electron transfer process [5] have been proposed. Mechanisms involving $HS^{\bullet}$ sulfhydryl radicals formed by the direct attack of H_2S by holes or by reaction with $OH^{\bullet}$ radicals, molecular oxygen or directly the $OH^{\bullet}$ radicals have been proposed to take part in the H_2S oxidation into sulfates [4–6,9–11,13]. Based on IR spectroscopy investigation, Kataoka et al. proposed that adsorbed SO_2^- may be a possible reaction intermediate and could provide a clue as to the reaction pathway, which might help to unravel the entire eight-electron transfer process [5]. Strategies have been recently elaborated for developing low SO_2 selectivity photocatalytic material, *i.e.* for minimizing the release of the hazardous SO_2 pollutant to the gas phase and for delaying its formation in comparison to the sulfate production. It included the design of sol–gel TiO_2, TiO_2/M-MCM-41 (M = Cr, Ce) mesoporous systems or hybrid TiO_2–SiM_gO_x composites for combined chemisorption and photocatalytic removal [12]. Cheap, lightweight and easily shaped UV-transparent polymeric supports for TiO_2 nanoparticle thin films were also studied as alternative to borosilicate glass or opaque monoliths [9].

The aim of this paper is to report on a parametric study of the H_2S photocatalytic oxidation under UV-A illumination over the TiO_2 P25 reference, not available up to now, in terms of influence of the photocatalyst weight, the total flow rate, the relative humidity, the temperature and the UV-A irradiance. Whereas such a parametric study was already available for the photocatalytic degradation of many liquid phase pollutants such as dyes or pesticides, or of

* Corresponding author. Tel.: +33 36885 2736; fax: +33 36885 2761.
E-mail address: vkeller@chimie.u-strasbg.fr (V. Keller).

0926-3373/$ – see front matter © 2011 Elsevier B.V. All rights reserved.
doi:10.1016/j.apcatb.2011.12.014

many gas phase hydrocarboned VOCs, no systematic results were established up to now for the H_2S photocatalytic oxidation, except scarce works of Portela et al. [9,13]. Surface characterization and regeneration treatments were also investigated.

2. Experimental

2.1. Characterization techniques

Thermal gravimetry analysis (TGA) was performed using a TGA 5000 thermo-analyzer. Each sample was placed in a platinum crucible and heated from room temperature to 900 °C with a heating rate of 20 °C/min, using a 20/80 vol.%/vol.% O_2/N_2 mixture at a flow rate of 35 mL/min.

X-ray photoelectron spectroscopy (XPS) surface characterization was performed on a ThermoVG Scientific apparatus equipped with a Al K_α (1486.6 eV) source (pass energy of 20 eV). All the spectra were decomposed assuming several contributions, each of them having a Doniach–Sunjic shape [14] and a Shirley background subtraction [15]. The sulfur-to-titanium (S/Ti) surface atomic ratios have been calculated using the sensitivity factors, as determined by Scofield [16]. The subtraction of the energy shift due to electrostatic charging was determined using the contamination carbon C 1s band at 284.6 eV as reference.

Infrared Fourier transform spectroscopy (IRTF) was carried out with a Nicolet analyzer working in the transmittance mode using a 90 wt.% anhydrous KBr pellet.

The light transmission through the photocatalytic coating was directly measured on the TiO_2-coated photoreactor, by comparing incident and transmitted light irradiance through the coating inside the reactor, using a wideband RPS900-W rapid portable spectroradiometer (International Light Technology).

2.2. Experimental device and procedure

The photocatalytic reaction was carried out in a 270 mm length single pass annular Pyrex reactor made of two coaxial tubes (*i.d.* 28 mm and *e.d.* 30 mm), between which the reactant mixture was passing through. Details concerning both reactor and device can be found elsewhere [17]. 10–800 mg of photocatalytic material, corresponding to a surface density of 0.04–3.37 mg/cm^2, was evenly coated on the internal side of the 30 mm diameter external tube by evaporating a catalyst-containing aqueous suspension to dryness. The catalyst coated reactor was finally dried at 110 °C for 1 h in air.

Except for tuning the H_2S and the water vapor concentrations, the composition of the reactant feed was H_2S (15 ppm, corresponding to 0.023 mg of H_2S per m^3), air (92 vol.%), and balanced He, fed through mass-flow controllers with a total flow ranging from 100 to 980 mL/min, corresponding to total flow rates and residence times within the 0.7–6.86 cm/s and 38–3.9 s ranges, respectively. For tuning the water vapor content, the relative humidity was defined by considering 100% of relative humidity as the saturated vapor pressure of water at 25 °C and pressure of 1 atm, corresponding to about 24 Torr. A cylindrical furnace or a water-cooling system surrounding the photoreactor was used for tuning the temperature of the tests in the 22–160 °C range. The tests were mainly conducted at 500 mL/min total flow rate, with a 3.5 cm/s flow rate and a 7.6 s residence time, in dried conditions. Before the photocatalytic reaction, the catalyst was first exposed to the polluted air stream with no illumination until dark-adsorption equilibrium was reached. Afterwards the UV illumination was switched on. Illumination was provided by commercially available 8 W and 15 W blacklight tubes (Philips TL8W/08 BLB F8T5 and Sylvania T5/BL350), with a spectral peak centered around 380 nm, located inside the inner tube of the reactor. H_2S and SO_2 were analyzed *on-line* every 3 min by a pulsed flame photometric detector (PFPD) coupled to a CP-Sil 5 CB column on a gas chromatograph (Varian 3800).

The efficiency of the depollution process was expressed in terms of H_2S conversion, of SO_2 selectivity – that is expected as low as possible since SO_2 remained a hazardous and unwanted gaseous by-product – and of sulfur removal in the gas phase, according to Eqs. (1)–(3). Depending on the test conditions, the duration at total sulfur removal could be also reported.

$$C_{H_2S}(\%) = \frac{[H_2S]_{in} - [H_2S]_{out}}{[H_2S]_{in}} \times 100 \quad (1)$$

$$S_{SO_2}(\%) = \frac{[SO_2]_{out}}{[H_2S]_{in} - [H_2S]_{out}} \times 100 \quad (2)$$

$$\text{Sulfur removal } (\%) = \left(1 - \frac{[H_2S]_{out} + [SO_2]_{out}}{[H_2S]_{in}}\right) \times 100 \quad (3)$$

Regeneration of the photocatalysts was performed *ex situ* by washing the used photocatalysts under mechanical stirring in an aqueous or a 0.01 M NaOH solution (20 mL) at 25 °C or 50 °C for 5 h. After water washing, the samples were filtered and dried at 110 °C overnight, before being coated again inside the reactor or characterized.

3. Results and discussion

3.1. Influence of TiO_2 surface density

Fig. 1A–C shows the on-stream evolution of H_2S conversion and SO_2 selectivity obtained on TiO_2 P25 as a function of the surface density, as well as the performances obtained after 5.5 h under stream. The influence of the surface density on both durations with no H_2S release and no SO_2 release – this latter corresponding thus to the duration at total sulfur removal – is summarized in Fig. 2. The general behavior of the photocatalyst was characterized by an on-stream deactivation, with a quicker and more pronounced decrease in the H_2S conversion for low TiO_2 surface densities. Increasing the surface density led to maintain a complete H_2S conversion for longer durations before deactivation occurred with time on stream, and to delay the appearance of SO_2 in the outlet flow. The SO_2 selectivity seems to stabilize at a higher value with increasing density, however, at the highest surface densities tested, due to the delay in SO_2 appearance, the SO_2 selectivity was still increasing after 5.5 h of time on stream. Thus, with 15 ppm of H_2S inlet concentration, both H_2S conversion and SO_2 selectivity increased with increasing the TiO_2 surface density. For densities higher than 0.44 mg/cm^2, the H_2S conversion reached 100% and the SO_2 selectivity was strongly decreased. One should note that the non steady-state of both SO_2 selectivity and sulfur removal after 5.5 h of time on stream at the two highest TiO_2 surface densities, might be the reason of the observed behavior for high TiO_2 surface densities.

Thus, to confirm the influence of the surface density parameter, the reaction conditions have been tightened, with an increased inlet H_2S concentration of 100 ppm and a total flow of 1 L/min (Fig. 3). This led to determine the optimal TiO_2 P25 surface density for the degradation of H_2S at 2.53 mg/cm^2 (*i.e.* 600 mg of TiO_2), with the linear increase in H_2S conversion with increasing the surface density, before asymptotically stabilizing at 80%. This behavior as a function of the photocatalyst mass was in agreement with that usually reported for the photocatalytic oxidation of VOCs, with a first linear increase in the activity with the surface density, due to the increase in the amount of TiO_2: this corresponds to the case for which all the particles are totally illuminated [18]. For higher catalyst amounts, a screening effect of excess particles occurs, which masks part of the photosensitive semiconductor surface, due to the limited penetration thickness of UV-A light (Fig. 4). Also, with increasing the photocatalytic coating thickness, limitation of the reactant

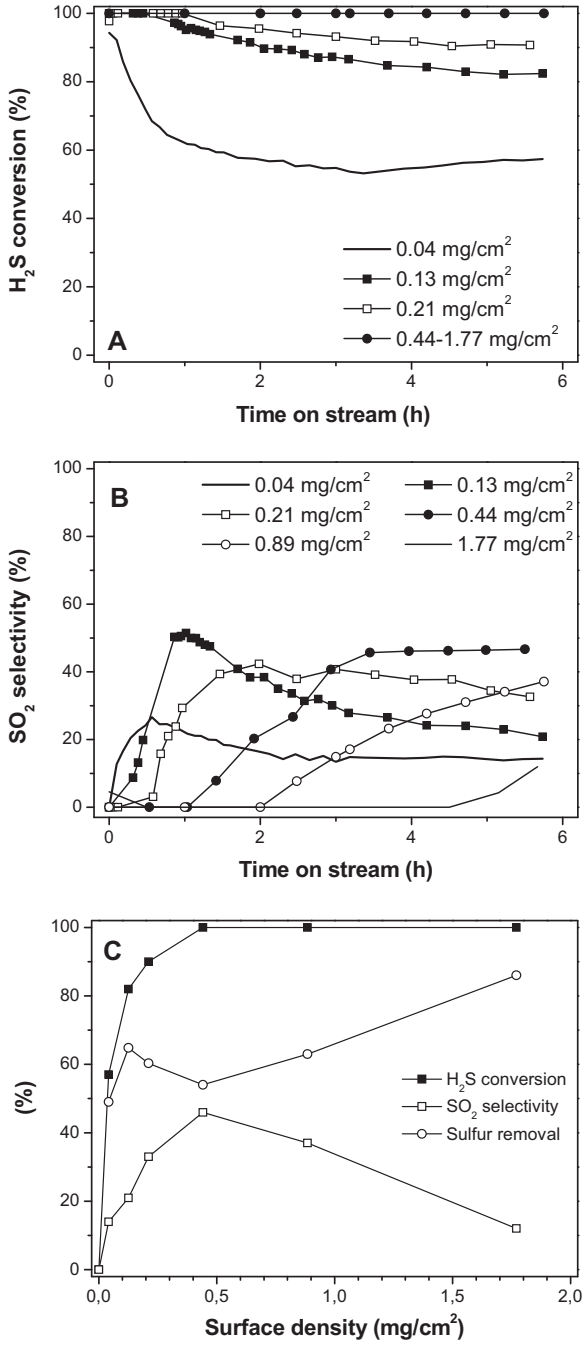

Fig. 1. On-stream evolution of (A) H_2S conversion and (B) SO_2 selectivity on TiO_2 P25 as a function of the surface density in the 0.04–1.77 mg/cm^2 range. (C) H_2S conversion, SO_2 selectivity and sulfur removal obtained after 5.5 h of test. SO_2 selectivity and sulfur removal were stable except for the two highest TiO_2 surface densities. Test conditions: [H_2S] = 15 ppm, total flow of 500 mL/min.

diffusion within the coating occurred, and as a result, the TiO_2 particles that were the most weakly illuminated, were also subjected to the lowest H_2S concentration, so that the deepest internal TiO_2 layers displayed the lowest reaction rate [19].

3.2. Surface analysis and surface active sites

First, it should be pointed out here that, due to light penetration and reactant diffusion across the TiO_2 coating, the H_2S conversion was not homogeneous along the coating thickness. As a result, the surface properties of the used photocatalyst (*e.g.* the surface

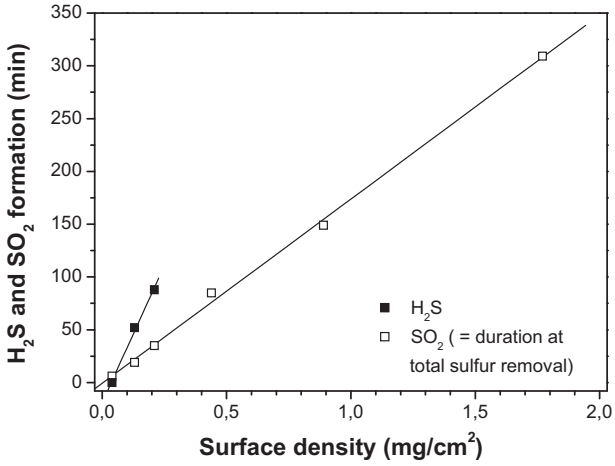

Fig. 2. Durations with no H_2S release and no SO_2 release (corresponding thus to the duration at total sulfur removal) on TiO_2 P25 as a function of the surface density in the 0.04–1.77 mg/cm^2 range. Test conditions: [H_2S] = 15 ppm, total flow of 500 mL/min.

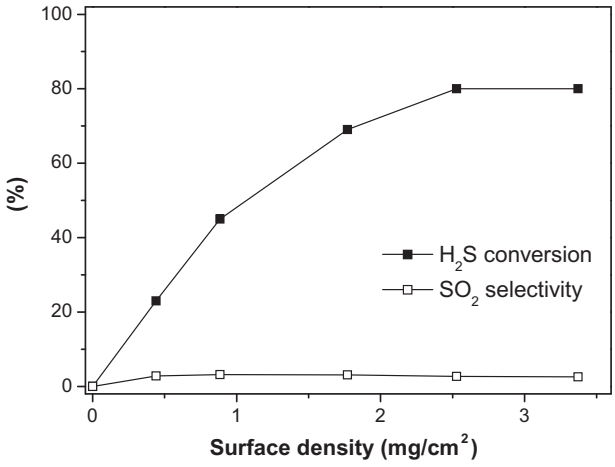

Fig. 3. H_2S conversion and SO_2 selectivity obtained on TiO_2 P25 after 5.5 h of test, as a function of the surface density in the 0.44–3.37 mg/cm^2 range. Test conditions: [H_2S] = 100 ppm, total flow of 1 L/min. Here, SO_2 selectivity was stable as a function of time on stream.

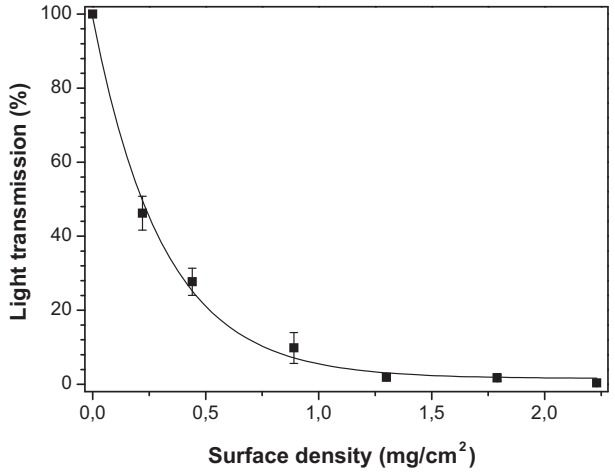

Fig. 4. Light transmission as a function of the surface density of the TiO_2 P25 coating. Light transmission experimental data have been modeled by a first order decreasing exponential.

sulfate amount) were depending on the photocatalyst location within the coating (deep internal or external layers). Thus, recovering the whole used photocatalyst after test led globally to average the characterization data, with a stronger influence in the case of high surface density tests. In the case of XPS characterization of used photocatalysts especially, this inhomogeneity within the coating led to a gradient in terms of S/Ti surface atomic ratio and of relative contents of surface oxygenated phases along the coating thickness, with unfortunately no access to such real data. Therefore, after test, the calculated values derived from XPS spectra were considered as *averaged* S/Ti surface atomic ratios and *averaged* relative contents of surface oxygenated phases.

Fig. 5A–B shows both Ti 2p and O 1s regions of the XPS spectra recorded on fresh TiO_2 P25 and that after 25 h of reaction. The Ti 2p spectra of the fresh sample shows the doublet related to the Ti $2p_{3/2}$–Ti $2p_{1/2}$ spin–orbit components of Ti^{4+} surface species, at 458.3 eV and 464.0 eV respectively, and no contribution attributed to Ti^{3+} species was detected, indicating the presence of few surface defects [20]. Performing the reaction at a surface density of 0.21 mg/cm^2, led to the appearance of a higher energy doublet contribution at 459.7–465.5 eV, assigned to the formation of a Ti—S binding, already reported by Grandcolas [21] for titanium inserted inside a multi-walled TiO_2 nanotube – so with a probably different electronic environment – after the UV-A photocatalytic degradation of diethylsulfide (DES). By contrast, similarly to Grandcolas, no reduction of Ti^{4+} to Ti^{3+} was observed during the reaction. A slight shift to higher binding energy of Ti^{4+} from 458.3 eV to 458.7 eV, *i.e.* +0.4 eV, was observed after test, and attributed to the increase in effective positive charge around Ti^{4+} surface species, suggesting the direct coordination of titanium atoms to strongly electron-withdrawing SO_4 centers and the existence of an electron transfer from TiO_2 to sulfate anions. A similar 0.2–0.5 eV upward shift of Ti^{4+} 2p binding energies, depending on the sulfation conditions, was observed by Barraud et al. on sulfated titania photocatalysts [22]. It was suggested that the resulting possible titanium → sulfate electronic transfer was beneficial to the photogenerated charge separation, and thus to the photocatalytic yield. Since the deepest internal TiO_2 layers were the most weakly illuminated and displayed the lowest reaction rate, XPS investigation was also carried out on the photocatalyst after test at a lower surface density of 0.04 mg/cm^2, in order to artificially concentrate the sulfates in the analyzed sample, and the Ti 2p contribution assigned to the Ti—S binding was more markedly observed, with a relative content of 10% *vs.* only 6% after test at a surface density of 0.21 mg/cm^2.

The O 1s spectra obtained on the fresh TiO_2 P25 was characterized by three contributions, at 529.4 eV, 531.5 eV and 533.3 eV, attributed to O—Ti binding in TiO_2 network, Ti—O—H binding corresponding to hydroxyl surface groups and oxygen from residual water molecules adsorbed at the surface, respectively. After test at 0.21 mg/cm^2, an additional contribution arising at 532.0 eV was observed, assigned to oxygen bonded to the central atom of sulfur within sulfate species attributed to the O—S binding [21,23,24]. The main peak assigned to O—Ti binding in TiO_2 network was shifted from 529.4 eV to 529.8 eV, *i.e.* +0.4 eV. This could result from the presence of the electron-withdrawing sulfate on the Ti^{4+} center and thus from Ti^{4+} to sulfate anion electron transfer, that could indirectly lead to an electron donation from the oxygen of O—Ti binding to the Ti^{4+} center.

After photocatalytic test at 0.21 mg/cm^2, the S 2p region of the XPS spectra shown in Fig. 5C exhibited a broad signal, composed of the doublet related to the S $2p_{3/2}$–S $2p_{1/2}$ spin–orbit components at 168.2 eV and 169.6 eV, assigned to surface S^{6+} sulfate species [25]. One could also not exclude that the S 2p spectra could be slightly enlarged by the presence of surface polysulfate species which could result from a partial and local polymerization of surface sulfates, or

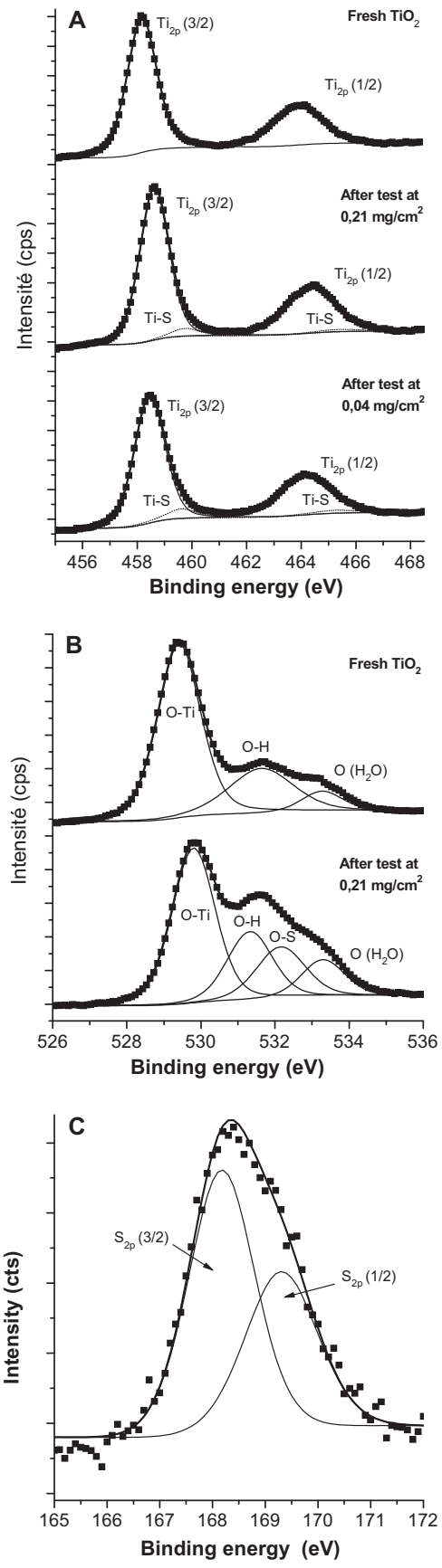

Fig. 5. XPS spectra of (A) titanium Ti 2p of TiO_2 P25, fresh and after 25 h of test at 0.21 mg/cm^2 and 0.04 mg/cm^2, (B) oxygen O 1s of TiO_2 P25, fresh and after 25 h of test at 0.21 mg/cm^2 and (C) sulfur S 2p after 25 h of test at 0.21 mg/cm^2.

Table 1
Averaged relative content of the different surface phases and averaged S/Ti surface atomic ratios derived from XPS data. The surface properties of used TiO_2 being not homogeneous along the coating thickness, the averaged nature of the XPS data resulted from the recovering of the whole photocatalyst after test.

Sample	O—Ti^{4+}	O—H	H_2O	O—S	S/Ti
Fresh TiO_2 P25	67	26	7	-	0
TiO_2 P25 after test at 1.77 mg/cm^2	56	23	8	13	0.17
TiO_2 P25 after test at 0.21 mg/cm^2	48	22	11.5	18	0.22

by the presence of sulfates with different coordination modes to Ti^{4+}, which could result in a change in the electronic environment of the sulfur atom. Indeed, FTIR spectra in Fig. 6 evidenced vibration bands at 1210 cm^{-1}, 1145 cm^{-1} and 1050 cm^{-1}, as also reported by Canela et al. [4] and Han et al. [24], and attributed to sulfates with mono- and bi-chelated coordination modes to Ti^{4+}.

The averaged relative contents of oxygenated phases at the surface of TiO_2 P25, fresh and after tests at low (0.21 mg/cm^2) and high (1.77 mg/cm^2) surface density, are derived from XPS study (Table 1). Whatever the surface density, the averaged —OH relative content remained unchanged compared to fresh TiO_2 at 22–26%, while the averaged O—Ti^{4+} relative content decreased from 67% for the fresh TiO_2 down to 56% and 48% after test at 0.21 mg/cm^2 and 1.77 mg/cm^2, respectively, together with the simultaneous increase in the averaged O—S relative content up to 13% and 18%, respectively. In addition, the averaged S/Ti surface atomic ratio was higher at 0.21 mg/cm^2 compared to 1.77 mg/cm^2, being calculated at 0.22 and 0.17, respectively. Thus, increasing the TiO_2 coating thickness – so that only a part of it was activated by light – led to a weaker decrease in the averaged O—Ti^{4+} relative content, a weaker increase in the averaged O—S relative content and a weaker averaged S/Ti surface atomic ratio when compared to those obtained with a thinner coating, for which the whole coating was activated by light. This confirmed the active role played by the external layers of the TiO_2 coating when compared to the deepest ones, in agreement with the light transmission record through the TiO_2 film, lower than 10% for a 1.77 mg/cm^2 surface density. Thus, the deepest internal TiO_2 layers did not play any significant role in the photocatalytic oxidation of H_2S.

However, when increasing the surface density of the coating, the strong impact of the deepest – and thus weakly or even non illuminated – internal layers, led to propose that internal layers could act for adsorbing SO_2 and H_2S, and thus for artificially increasing the H_2S and SO_2 residence time within the photocatalytic coating and

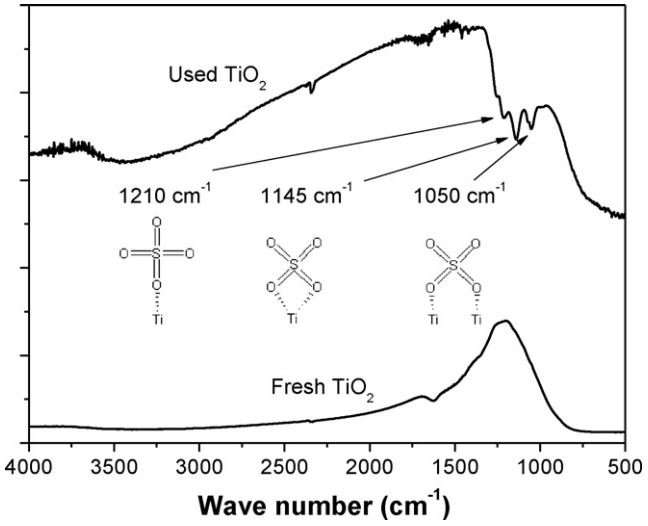

Fig. 6. FTIR analysis of fresh TiO_2 P25 and TiO_2 P25 after photocatalytic test.

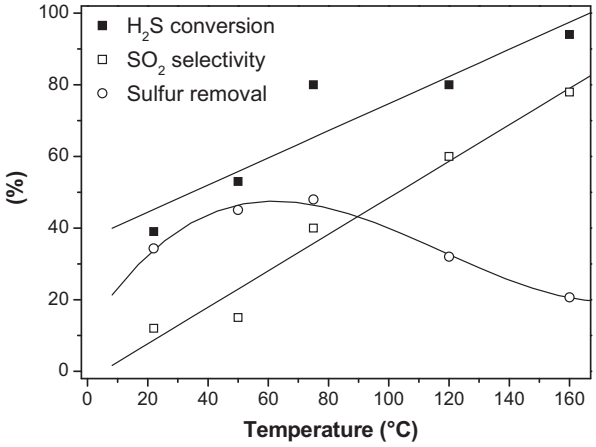

Fig. 7. Influence of the temperature on the H_2S conversion, SO_2 selectivity and sulfur removal obtained on TiO_2 P25 after 5.5 h of test. Test conditions: $d(TiO_2)$ = 0.04 mg/cm^2, [H_2S] = 15 ppm, total flow of 500 mL/min.

positively retarding the release of the unwanted SO_2 by-product. Such a role of non-illuminated TiO_2 particles located deep inside the coating has been already put forward by Salem et al. in the gas phase photocatalytic removal of monoterpenes [26]. Increasing the surface density from 1 mg/cm^2 till high levels of 14.3 mg/cm^2, – so with thicknesses highly above usual UV-A penetration depth – the authors have observed an unexpected increase in the terpene removal efficiency and a strongly reduced photocatalyst deactivation.

3.2.1. Surface active sites

XPS and FTIR studies detailed above led to put forward that O—Ti^{4+} surface sites would be the active sites for the H_2S photocatalytic oxidation. This differs from results obtained by Grandcolas on anatase/rutile mixed phase TiO_2, who proposed that —OH surface sites could be considered as the active sites, but in the case of the vapor phase photocatalytic oxidation of DES [21]. By contrast he previously also concluded to the activity of O—Ti^{4+} surface active sites towards DES over one-dimension WO_3-modified titanate nanotubes. Here, by analogy to water molecule adsorption occurring dissociatively on non-hydroxylated TiO_2 and molecularly on OH-rich surfaces, the adsorption of H_2S would take place molecularly on hydroxylated TiO_2 P25 particles on Ti^{4+} sites through the central sulfur atom of H_2S. This was also proposed by Yanxin et al. during the study of H_2S and SO_2 adsorption on medium surface area TiO_2, obtained by hydrolysis of titanium sulfate with final calcination at 500 °C [27], *i.e.* closer to real reaction conditions than when adsorption studies were performed over well-defined non-hydroxylated (1 1 0) TiO_2 surfaces. In addition, it has been reported that the formation of hydrogen binding with —OH groups through S—H groups of H_2S molecules could not easily occur, being more favorable in very basic media [28]. One could not exclude that adsorption of H_2S *via* —OH groups could occur when the Ti^{4+} adsorption sites would be fully saturated.

3.3. Influence of temperature

Fig. 7 shows the influence of the temperature in the 20–160 °C range on the stabilized H_2S photodegradation performances. Increasing the temperature led to an increase in the H_2S conversion from 40% up to 94%, together with a strong increase in the SO_2 selectivity from 12% to 78%, so that the sulfur removal curve displayed a volcano shape with the temperature, with a maximum at 47–48% at about 50–75 °C. This temperature dependence could be mainly attributed to changes in the adsorption

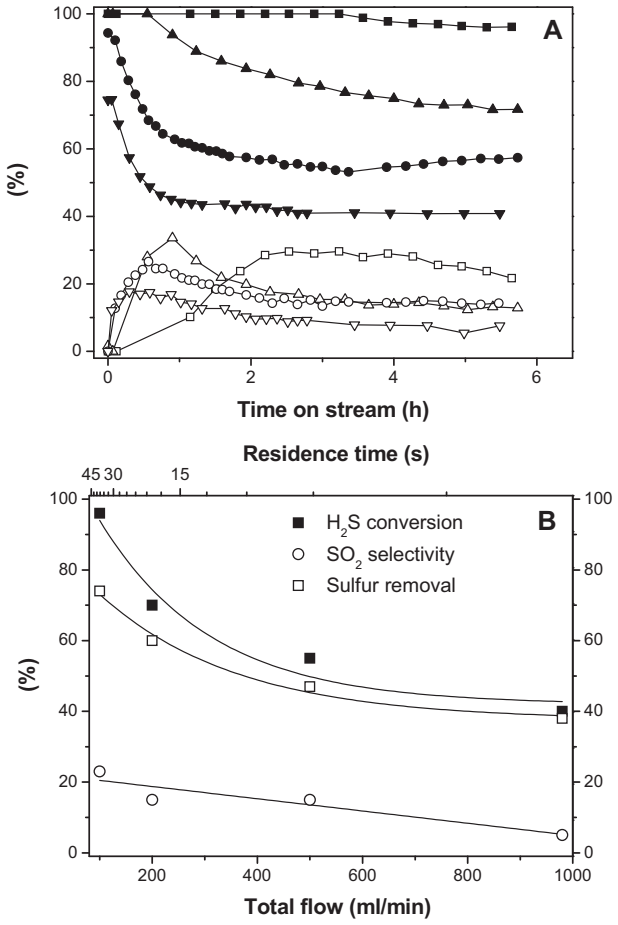

Fig. 8. (A) Influence of the total flow rate on the evolution with time on stream of H_2S conversion (filled symbols) and SO_2 selectivity (empty symbols). (■,□) 100 mL/min (●, ○) 200 mL/min (▲, △) 500 mL/min and (▼, ▽) 980 mL/min. (B) Influence of the total flow rate on the H_2S conversion, the SO_2 selectivity and the sulfur removal after stabilization at t = 5.5 h. Test conditions: $d(TiO_2)$ = 0.04 mg/cm^2, [H_2S] = 15 ppm.

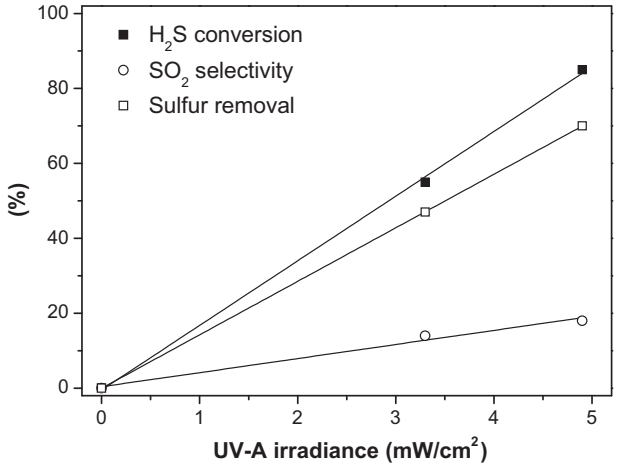

Fig. 9. Influence of the UV-A irradiance on the H_2S conversion, SO_2 selectivity and sulfur removal obtained on TiO_2 P25 after 5.5 h of test. Test conditions: $d(TiO_2)$ = 0.04 mg/cm^2, [H_2S] = 15 ppm, total flow of 500 mL/min.

equilibrium of involved species, as suggested by Portela et al. [9]. They observed also a linear relationship between H_2S conversion and temperature. Twesme et al. [29] and Zorn et al. [30] have also reported a similar temperature dependence, but not for temperatures higher than 77 °C, for which a decrease in the light intensity with increasing the temperature was pointed out for explaining a down-shift of the conversion compared to linearship. In the present study, no irradiance decrease was measured with increasing the temperature, so that the linear relationship was still observed for elevated temperatures. Here, at low temperature, considering a SO_2-through reaction mechanism, the adsorption of H_2S, as well as that of SO_2 was favored, so that the SO_2 selectivity remained low at 12%, with mainly sulfate formation, responsible for the photocatalyst deactivation. By contrast, at high temperature (120–160 °C), SO_2 desorption was favored and its possible subsequent re-adsorption was strongly unfavored, so that the SO_2 selectivity was very high. One could also not exclude that some impurity traces (such as iron) in TiO_2 P25 samples could contribute at 120–160 °C to the increase in the H_2S conversion by thermal catalysis.

This behavior with the temperature confirmed the interest of using photocatalysis in the medium temperature range of 20–80 °C [18,31], which is practically the operation temperature in nowadays and in future photocatalysis depollution applications.

3.4. Influence of flow rate

The influence of the flow rate on the H_2S conversion, the SO_2 selectivity and the sulfur removal is shown in Fig. 8. Whatever the flow rate, TiO_2 P25 displayed a similar behavior, with an initial deactivation before stabilizing after few hours (Fig. 8A). However, the deactivation was stronger and quicker with increasing the flow rate. At low flow rate, the number of active sites available was not limiting and the conversion was less influenced by sulfate deposition, while at high flow rates, adsorption of H_2S and intermediate molecules could saturate the available active sites, thus causing a rapid decrease in conversion. In Fig. 8B, H_2S conversion and SO_2 selectivity decreased with increasing the flow rate, the conversion in a strongly higher extent than the selectivity, so that the sulfur removal was largely more efficient at the 100 mL/min flow rate.

3.5. Influence of UV-A irradiance

At 3.3 mW/cm^2 and 4.9 mW/cm^2 UV-A irradiance, TiO_2 P25 displayed a similar behavior, with an initial deactivation before stabilizing after few hours on stream (not shown). Fig. 9 shows the influence of the irradiance on the stabilized performances. Increasing the irradiance from 3.3 mW/cm^2 to 4.9 mW/cm^2 resulted in an increase in the H_2S conversion and in a lesser extent in the SO_2 selectivity, so that globally the sulfur removal was also enhanced. Linear relationships were observed, in agreement with works reported by Herrmann for gas or liquid phase organic molecule degradation (such as VOCs or dyes), in which the author has estimated that the linear to square root regime change occurs at about 25 mW/cm^2 irradiance in laboratory conditions, and below which the photogenerated holes could be considered as the rate limiting active species [31].

3.6. Influence of relative humidity

First, whatever the relative humidity, the photocatalyst displayed a similar behavior than under dry conditions, with an initial deactivation before stabilizing after few hours on stream (not shown). Fig. 10 shows the influence of relative humidity on the performances, and that the highest H_2S conversion and the lowest SO_2 selectivity, and therefore the best sulfur removal, were obtained in the absence of humidity. Indeed, the low content of 10% in relative humidity already caused the change in both H_2S conversion and SO_2 selectivity, from 56% and 14%, to 35% and 27%, respectively. This resulted in a drastic decrease in the sulfur removal rate from 48%

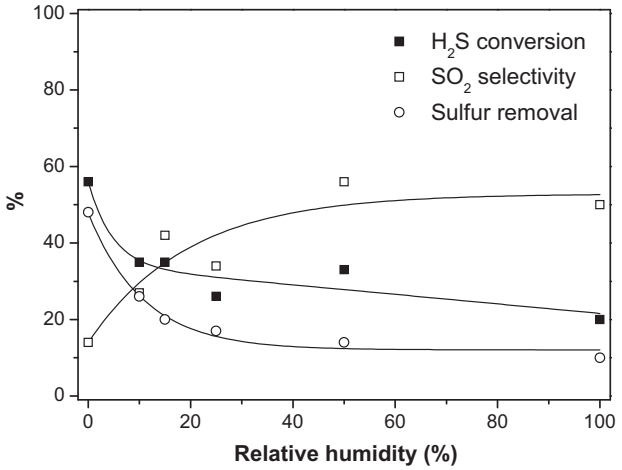

Fig. 10. Influence of the relative humidity on the H_2S conversion, SO_2 selectivity and sulfur removal obtained on TiO_2 P25 after 5.5 h of test. Test conditions: $d(TiO_2) = 0.04\ mg/cm^2$, $[H_2S] = 15$ ppm, total flow of 500 mL/min.

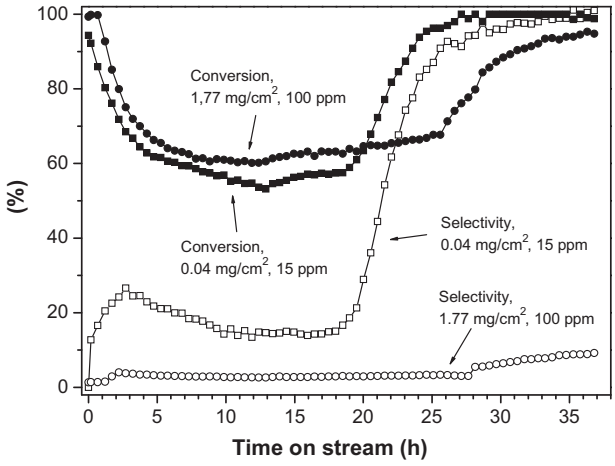

Fig. 11. Long-term evolution as a function of time on stream of the H_2S conversion and the SO_2 selectivity obtained at a surface density of 0.04 mg/cm^2 ($[H_2S] = 15$ ppm) and 1.77 mg/cm^2 ($[H_2S] = 100$ ppm). Test conditions: total flow of 500 mL/min.

down to 26%. H_2S photodegradation even took place at 100% relative humidity, although the performances were strongly affected, with residual H_2S conversion and SO_2 selectivity of 20% and 50%, respectively, corresponding to a low sulfur removal of 10%.

In the presence of water, considering that water molecules adsorb on the TiO_2 surface through —OH surface groups whereas H_2S molecules adsorb in priority on Ti^{4+} sites, one cannot argue *stricto sensu* that adsorption competition occurred, *i.e.* competition towards a single surface active site. However, competition between H_2O and H_2S molecules could take place in the sense of restricting the H_2S molecule access to Ti^{4+} sites, due to the partial or complete formation of layers of water molecules on the surface of TiO_2. The usually positive formation of oxidative OH• radicals from adsorbed water with subsequent reaction with H_2S, seems here to be negatively compensated by the restricted access of H_2S molecules towards active sites. When the relative humidity increased significantly, this decrease in the accessibility of sites also resulted from the need for H_2S molecules to diffuse into water layers. Taking into account the moderate solubility of H_2S in water, *i.e.* about 4000 mg/L and 3200 mg/L at 20 °C and 30 °C, respectively [32], the capacity of H_2S to diffuse into water molecules layers could also explain the maintain of a residual activity, even at a low level, in the presence of a very high relative humidity.

In the absence of relative humidity, there is, at least initially at the beginning of the test, no competitive adsorption for active sites, so that the H_2S conversion was high. Taking into account a SO_2-through reaction mechanism as well as the favored adsorption of SO_2 on —OH surface groups as reported by Baltrusartis et al. [33], one could assume that desorption of SO_2 intermediate from Ti^{4+} sites could be unfavored due to its stabilization through directly neighboring —OH groups. Increasing the humidity with adsorption of H_2O molecules on the —OH groups could thus weaken this stabilization, and therefore promote SO_2 desorption, resulting in an increase in the SO_2 selectivity.

3.7. Photocatalyst reactivation

Fig. 11 shows the long-term evolution of the H_2S conversion and the SO_2 selectivity at a surface density of 0.04 mg/cm^2 ($[H_2S] = 15$ ppm) and 1.77 mg/cm^2 ($[H_2S] = 100$ ppm). At 0.04 mg/cm^2, the usual short-term behavior with initial deactivation and further stabilized performances was followed by an increase in the H_2S conversion up to 100% together with a progressive turn of the SO_2 selectivity to 100%. This "reactivation" behavior was also observed at the high 1.77 mg/cm^2 density, with the necessity here to tight the reaction conditions by increasing the inlet H_2S concentration to 100 ppm. Here, the increase in SO_2 selectivity to reach 100% was delayed and shifted to longer test durations.

3.8. Reaction mechanism hypothesis

General reaction pathways leading to the formation of the detected reaction products, *i.e.* SO_2 in the gas phase and sulfates at the surface, is shown in Scheme 1. They could be described by several competitive reaction mechanisms.

After adsorption of H_2S, the reaction pathways (**1**) corresponds to the partial oxidation of H_2S into SO_2, which could occur through the HS• sulfhydryl radical formation. The HS• sulfhydryl radical could be formed either by the direct attack of H_2S by holes, similarly to the proposition of Canela et al. [34] and Vorontsov et al. [35] for other sulfur-containing organic molecules, according to Eq. (4), or by reaction with OH• hydroxyl radicals formed by the oxidation of adsorbed water by the holes, according to Eq. (5) [11].

$$H_2S_{ads} + h^+ \rightarrow H_2S^{\bullet +}_{ads} \leftrightarrow HS^{\bullet}_{ads} + H^+ \quad (4)$$

$$H_2S_{ads} + OH^{\bullet}_{ads} \rightarrow HS^{\bullet}_{ads} + H_2O_{ads} \quad (5)$$

The redox potential of sulfides is about +1.8 V with respect to the normal hydrogen electrode and lower than the redox potential of photogenerated holes in TiO_2 (+3 V) [9]. It can be proposed that HS radicals further react with oxygen according to a similar reaction than that proposed by Vidal et al. for the degradation of sodium N-methyldithiocarbamate ($CHNNaS_2$, a fungicide known as Vapam®) [36], so that HSOO• could be the possible precursor of adsorbed SO_2.

$$HS^{\bullet}_{ads} + O_{2,ads} \rightarrow HSOO^{\bullet}_{ads} \quad (6)$$

$$HSOO^{\bullet}_{ads} + O_{2,ads} \rightarrow SO_{2,ads} + HO^{\bullet}_{2,ads} \quad (7)$$

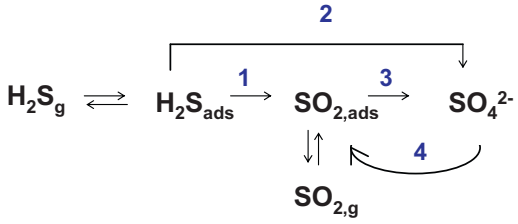

Scheme 1. General reaction pathways involving H_2S^{2-}, $S^{4+}O_2$ and $S^{6+}O_4{}^{2-}$.

Table 2
Influence of the *ex situ* washing conditions of the regeneration treatment on the H_2S conversion and the SO_2 selectivity obtained on TiO_2 P25, for a washing duration of 5 h and 20 mL of solvent. TGA was performed after 10 h of reaction. Reaction conditions: $d(TiO_2) = 0.21$ mg/cm^2, $[H_2S] = 15$ ppm, total flow of 500 mL/min.

Photocatalyst	H_2S conversion (%)	SO_2 selectivity (%)	Weight loss (%)
Fresh TiO_2 P25	87	30	1.5
Used TiO_2 P25	–	–	13.5
Used TiO_2 P25 after regeneration in water at 25 °C	50	60	4
Used TiO_2 P25 after regeneration in water at 50 °C	65	49	3.7
Used TiO_2 P25 after regeneration in 0.01 M NaOH at 25 °C	84	33	1.5
Used TiO_2 P25 after regeneration in 0.01 M NaOH at 25 °C	85	33	1.4

The possible reaction of $SO_{2,ads}$ with oxygen to form SO_3, which further is very rapidly hydrated into sulfuric acid due to its very hygroscopic nature, according to Eqs. (8)–(9), could explain the sulfate formation and the non-detection of SO_3 in the gas phase. This corresponded to the reaction pathway (**3**), recently also mentioned by Portela et al. [11].

$$SO_{2,ads} + \tfrac{1}{2}O_{2,ads} \rightarrow SO_{3,ads} \quad (8)$$

$$SO_{3,ads} + H_2O_{ads} \rightarrow H_2SO_{4,ads} \quad (9)$$

Alternatively, in terms of SO_2 adsorption and reaction, Baltrusartis et al. have recently reported that the adsorption of SO_2 could significantly take place on —OH surface groups for reacting into $SO^{2-}_{3,ads}$ and subsequently forming surface $SO_4{}^{2-}$ sulfates by reaction under illumination with highly reactive oxygen atoms resulting from O_2 dissociation [34]. The possible role of SO_2 or $SO_3{}^{2-}$ as adsorbed reaction intermediates was in agreement with XPS studies performed by Kako et al. over TiO_2-based photocatalysts after H_2S oxidation [7]. Indeed, the presence of adsorbed $SO_{2,ads}$ or $SO_{3ads}{}^{2-}$ was put forward by the authors to explain the appearance of a lower energy contribution in the XPS S 2p peak, beside the main usual sulfate contribution.

The reaction of adsorbed H_2S with $OH^\bullet$ hydroxyl radicals could be another reaction mechanism for the pathways (**1**) and (**2**), leading without any formation of the active $HS^\bullet$ sulfhydryl radical, to the formation of SO_2 and sulfates, respectively (Eqs. (10)–(11)).

$$H_2S_{ads} + 4OH^\bullet{}_{ads} \rightarrow SO_2 + 2H^+ + 2H_2O_{ads} \quad (10)$$

$$H_2S_{ads} + 8OH^\bullet{}_{ads} \rightarrow SO_4{}^{2-} + 2H^+ + 4H_2O_{ads} \quad (11)$$

Canela et al. have reported those mechanisms in their first study of H_2S photocatalytic degradation, in which they only observed sulfates as reaction products [4]. This process would here be directly in competition with the formation of the active sulfhydryl radical by reaction between H_2S and $OH^\bullet$ (Eq. (5)). $OH^\bullet$ radicals would be formed through the oxidation by holes, either of H_2O_{ads} or of —OH surface groups on TiO_2. However, the direct formation of sulfates would imply through an eight electron transfer and involved simultaneously eight $OH^\bullet$ radicals. Even if water molecules were formed as by-product of the H_2S oxidation, this mechanism seems defavorable with a dried inlet flow.

However, at high relative humidity condition, the formation of a water film at the surface of TiO_2, taking into account the possible solubility of H_2S in water, even if moderate, could lead to aqueous solution reaction mechanisms to take place, involving other oxidizing radicals (Eqs. (12)–(14)) such as *e.g.* $HSSH^{\bullet-}$ or $HSS^{\bullet 2-}$ dimeric species [37]. In addition, the reaction of $HS^\bullet$ with O_2 was reported to give $SO_2{}^{\bullet-}$ radical in such an acidic surface water, giving rise to SO_2 and $HO_2{}^\bullet$. This implies that SO_2 radical formation should be favored at high relative humidity, and could thus explain the increase in the SO_2 selectivity for increasing relative humidity.

$$HS^\bullet + HS^- \leftrightarrow HSSH^{\bullet-} \quad (12)$$

$$HS^\bullet \leftrightarrow S^{\bullet-} + H^+ \quad (13)$$

$$HSSH^{\bullet-} \leftrightarrow HSS^{\bullet 2-} + H^+ \quad (14)$$

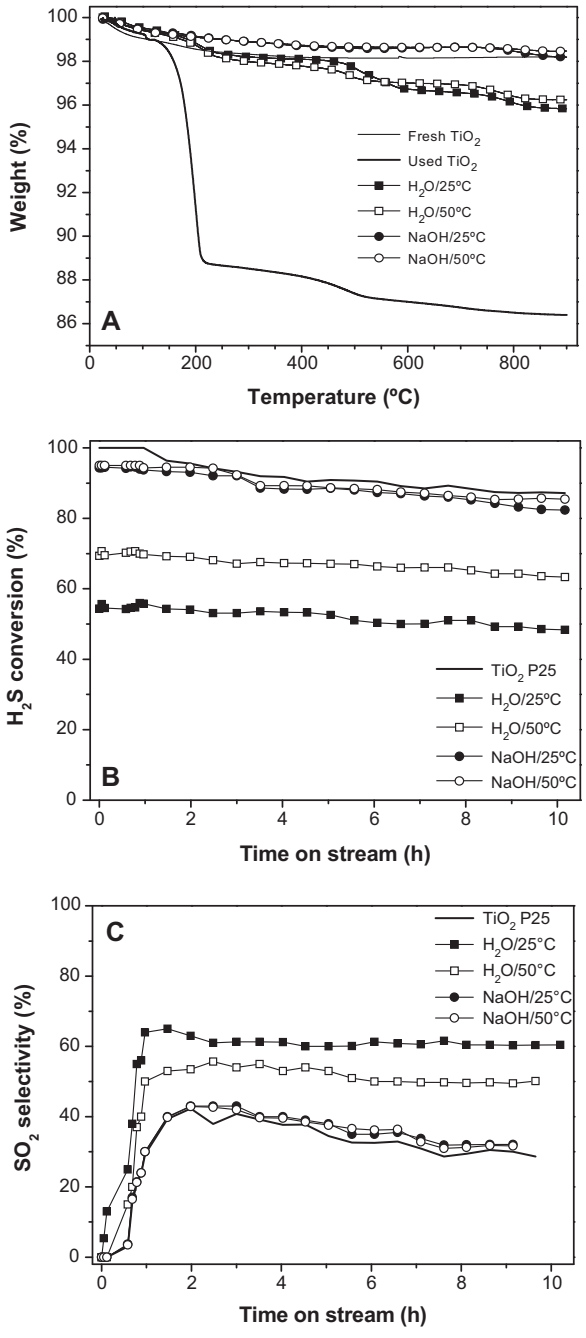

Fig. 12. Influence of the regenerative washing conditions on (A) the thermo gravimetry analysis (TGA) of photocatalysts, (B) the H_2S conversion and (C) the SO_2 selectivity as a function of time on stream. Test conditions: $d(TiO_2) = 0.21$ mg/cm^2, $[H_2S] = 15$ ppm, total flow of 500 mL/min.

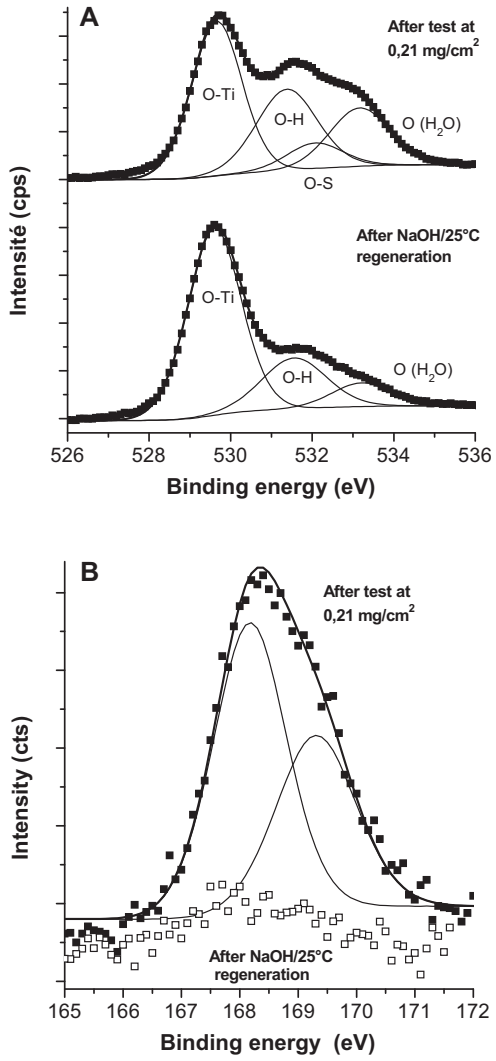

Fig. 13. XPS spectra of (A) oxygen O 1s and (B) sulfur S 2p, of the used TiO_2 P25 and of the used TiO_2 P25 after 0.01 M NaOH regeneration at 25 °C for 4 h. Test conditions: $d(TiO_2) = 0.21$ mg/cm^2, $[H_2S] = 15$ ppm, total flow of 500 mL/min, 25 h of test.

Finally, another reaction pathway (**4**) leading to the indirect formation of SO_2 and involving sulfate radicals could be put forward for explaining the long-term "photocatalyst reactivation" behavior shown in Fig. 11, with both increase in the H_2S conversion up to 100% together and progressive turn of the SO_2 selectivity to 100%. The reaction between surface SO_4^{2-} sulfates and photogenerated holes according to Eq. (15) [38] or even $OH^\bullet$ radicals [39], could lead to the formation of the adsorbed $SO_4^{\bullet-}$ sulfate radical, in agreement with the works of Portela [13].

$$h^+ + SO_4^{2-} \rightarrow SO^{\bullet-}_{4\,ads} \quad (15)$$

The sulfate radical has a high oxidative potential of +2.6 V, as reported by Malato et al. [40]. For long-term experiments, when the sulfate content of the surface strongly increase or even when the surface was saturated in sulfates, this reaction mechanism could be considered as being predominant, explaining the drastic change in performances, with a total H_2S conversion, but with total selectivity into SO_2. According to Abdullah et al. [39] and Portela [13], the reaction rate would however be lower than in the case of the oxidation of H_2S by photogenerated holes or by $OH^\bullet$ radicals. One could thus consider that a kind of equilibrium was established at the TiO_2 surface between the sulfate species and the SO_2 released to the gas phase.

The delay and shift to longer test durations of the photocatalyst "reactivation" observed in tighter reaction conditions for a high surface density of 1.77 mg/cm^2, *i.e.* with 100 ppm H_2S concentration, was probably due to the large number of adsorption sites available in the deepest layers of the coating. Although non-illuminated, they were impacting on the performances by delaying the SO_2 release.

3.9. Regeneration ability

Fig. 12 shows the H_2S conversion and the SO_2 selectivity obtained on TiO_2 P25 as a function of the regeneration treatment, as well as the corresponding thermogravimetric analyses performed on the different materials. The obtained results and the regeneration conditions are summarized in Table 2. One could note that using water as solvent only led to partially regenerate the sulfate loaded used photocatalyst, although increasing the temperature was favorable to the regeneration efficiency. Indeed, regenerating the TiO_2 P25 with water at 25 °C and 50 °C led to H_2S conversions of 50% and 65%, respectively, after 10 h of reaction, while the fresh photocatalyst still displayed a conversion of 87%. By contrast, whatever the temperature, a weakly basic washing with a 0.01 M NaOH aqueous solution was efficient to fully recover the activity of the TiO_2 P25, *i.e.* a conversion 85% compared to 87% for the fresh catalyst, the slight difference observed being attributed to the loss of few milligrams during the successive washing, drying and filtration steps.

Comparing the TGA signature of fresh, used and regenerated materials confirmed the efficiency of weakly basic aqueous washing when compared to a purely aqueous one (Fig. 12A). The sulfate removal was also evidenced by XPS analysis, with the disappearance of the S 2p doublet peak at 168.2–169.4 eV binding energy assigned to sulfate species, as well as of the O—S contribution at 532.0 eV binding energy within the O 1s peak, evidencing the refreshment of the photoactive TiO_2 surface (Fig. 13).

The efficiency of the regenerative basic washing treatment was explained by taking into account the isoelectrical point of TiO_2 P25, measured at 6.2. At basic pH, the TiO_2 surface was thus negatively charged as TiO^-, with a weakest affinity towards anions resulting in favoring the sulfate removal. By contrast, at more acidic pH, the positively charged TiO_2 surface as $TiOH_2^+$, with a strongest affinity towards sulfate anions, which were thus removed from the TiO_2 surface with more difficulty.

4. Conclusions

The influence of the main reaction parameters on the TiO_2 P25 photocatalytic behavior in the UV-A H_2S photocatalytic oxidation has been studied. TiO_2 suffered from on-stream deactivation, with a quicker and more pronounced decrease in the H_2S conversion for a low TiO_2 surface density. Increasing the surface density led to maintain a total H_2S conversion for longer durations before deactivation occurred, and to delay the appearance of SO_2 in the outlet flow. The deepest – and thus weakly or even non illuminated – internal layers of the TiO_2 coating have been proposed to act for adsorbing SO_2, and thus to positively retard the release of unwanted SO_2 and artificially increase the H_2S and SO_2 residence times within the photocatalytic coating. In addition to the key role of internal layers, unexpected result was the detrimental role of relative humidity, due the decrease in the accessibility of surface sites.

Photoholes, $HS^\bullet$ sulfhydryl and $OH^\bullet$ radicals were hypothized to be involved in the reaction mechanisms forming SO_2 in the gas phase and surface sulfates, whereas the $O—Ti^{4+}$ surface sites have been proposed to act as active sites for the H_2S oxidation. The role of the $SO_4^{\bullet-}$ sulfate radical has been put forward for explaining the unexpected change with time on stream in the photocatalyst

behavior, with the recovering of the H_2S conversion together with a switch into 100% SO_2 selectivity.

Tuning reaction conditions and TiO_2 coating could allow optimizing total sulfur removal efficiency, whereas regeneration of sulfate-deactivated TiO_2 and activity recovering by weakly basic sulfate washing, leads hoping in the design of an economically viable depollution process.

Acknowledgments

The authors thanks the EU for supporting this work, performed in the frame of the 6th FP EFFORTS European project – Effective Operation in Ports – FP6-031486. P. Bernhardt (LMSPC) is gratefully acknowledged for performing XPS characterization.

References

[1] B. Mills, Filtr. Sep. 2 (1995) 147.
[2] M. Tomar, T.H.A. Abdullah, Water Res. 28 (1994) 2545.
[3] K. Suzuki, S. Satoh, T. Yoshida, Denki Kagaku 59 (6) (1991) 521.
[4] M.C. Canela, R. Alberici, W.F. Jardim, J. Photochem. Photobiol. A: Chem. 112 (1998) 73–80.
[5] S. Kataoka, E. Lee, M.I. Tejedor-Tejedor, M.A. Anderson, Appl. Catal. B: Environ. 61 (2005) 159.
[6] S. Kato, Y. Hirano, T. Sano, K. Takeuchi, S. Matsuzawa, Appl. Catal. B: Environ. 57 (2005) 109–115.
[7] T. Kako, H. Irie, K. Hashimoto, J. Photochem. Photobiol. A: Chem. 171 (2005) 131–135.
[8] I. Sopyan, Sci. Technol. Adv. Mater. 8 (2007) 33–39.
[9] R. Portela, B. Sánchez, J.M. Coronado, R. Candal, S. Suarez, Catal. Today 129 (1–2) (2007) 223.
[10] R. Portela, M.C. Canela, B. Sánchez, F.C. Marques, A.M. Stumbo, R.F. Tessinari, J.M. Coronado, S. Suárez, Appl. Catal. B: Environ. 84 (3–4) (2008) 643.
[11] R. Portela, R.S. Suarez, S.B. Rasmussen, N. Arconada, Y. Castro, A. Duran, P. Avila, J.M. Coronado, B. Sanchez, Catal. Today 151 (2010) 64.
[12] S.B. Rasmussen, R. Portela, S. Suarez, J.M. Coronado, M.-L. Rojas-Cervantes, P. Avila, B. Sanchez, Ind. Eng. Chem. Res. 49 (2010) 6685.
[13] R. Portela, PhD Dissertation, Santiago de Compostela University, Spain, 2008.
[14] S. Doniach, M. Sunjic, J. Phys. C: Solid State Phys. 3 (2) (1970) 285.
[15] D.A. Shirley, Phys. Rev. B 5 (1972) 4709.
[16] J.H. Scofield, J. Electron. Spectrosc. Relat. Phenom. 8 (1976) 129.
[17] V. Keller, P. Bernhardt, F. Garin, J. Catal. 215 (2003) 129.
[18] J.M. Herrmann, Top. Catal. 34 (1–4) (2005) 49.
[19] D. Chen, F. Li, A.K. Ray, Catal. Today 66 (2001) 475.
[20] T. Kubo, A.A. Nakahira, J. Phys. Chem. 112 (2008) 1658.
[21] M. Grandcolas, PhD Dissertation, Strasbourg University, 2009.
[22] E. Barraud, F. Bosc, D. Edwards, N. Keller, V. Keller, J. Catal. 235 (2005) 318.
[23] S.M. Jung, P. Grange, Catal. Today 59 (2000) 305.
[24] S.T. Han, G.Y. Zhang, H.L. Xi, D.N. Xu, X.Z. Fu, X.X. Wang, Catal. Lett. 122 (2008) 106.
[25] J.F. Moulder, W.F. Stickle, P.E. Sobol, D.E. Bombon, Handbook of X-ray Photoelectron Spectroscopy, Perkin Elmer Corporation, Eden Prairie, Minesota, USA.
[26] I. Salem, N. Keller, V. Keller, Green Chem. 11 (2009) 966.
[27] C. Yanxin, J. Yi, L. Wenzhao, J. Rongchao, T. Shaozhen, H. Wenbin, Catal. Today 50 (1999) 39.
[28] G.C. Pimental, A.L. McClellan, The Hydrogen Bond, Freeman, London, 1960.
[29] T.M. Twesme, D.T. Tompkins, M.A. Anderson, T.W. Root, Appl. Catal. B: Environ. 64 (2006) 153.
[30] M.E. Zorn, D.T. Tompkins, W.A. Zeltner, M.A. Anderson, Appl. Catal. B: Environ. 23 (1999) 1.
[31] J.M. Herrmann, Catal. Today 24 (1995) 157.
[32] E.D. Weil, S.R. Sandler, M. Gernon, Kirk-Othmer Encyclopedia of Chemical Technology, J. Wiley and Sons, New York, 2006.
[33] J. Baltrusartis, M. Jayaweena, V.H. Grassian, J. Phys. Chem. C 111 (2011) 492.
[34] M.C. Canela, R.M. Alberici, R.C.R. Sofía, M.N. Eberlin, W.F. Jardim, Environ. Sci. Technol. 33 (1999) 2788.
[35] A.V. Vorontsov, E.V. Savinov, L. Davydov, P.G. Smirniotis, Appl. Catal. B: Environ. 32 (1–2) (2001) 11.
[36] A. Vidal, M.A. Martín Luengo, Appl. Catal. B: Environ. 32 (1–2) (2001) 1.
[37] T.N. Das, R.E. Huie, P. Neta, S. Padmaja, J. Phys. Chem. A 103 (27) (1999) 5221.
[38] R.W. Mattews, H.A. Mahlman, T.J. Sworski, J. Phys. Chem. 75 (9) (1972) 1265.
[39] M. Abdullah, G.K.C. Low, R.W. Matthews, J. Phys. Chem. 94 (17) (1990) 6820.
[40] S. Malato, J. Blanco, C. Richter, B. Braun, M.I. Maldonado, Appl. Catal. B: Environ. 17 (4) (1998) 347.